IOP Conf. Series: Journal of Physics: Conf. Series **791** (2017) 012019 doi:10.1088/1742-6596/791/1/012019

Investigation of point defects in HfO_2 using positron annihilation spectroscopy: internal electric fields impact

M Alemany[1,2,4], A Chabli[2], E Oudot[1,3,5], F Pierre[3], P Desgardin[4], F Bertin[3], M Gros-Jean[1] and M F Barthe[4]

[1] STMicroelectronics, 850 rue Jean Monnet, 38926 Crolles, France.
[2] Univ. Grenoble Alpes, INES, F-73375 Le Bourget du Lac, France, CEA, LITEN, Department of Solar Technologies, F-73375 Le Bourget du Lac, France
[3] Univ. Grenoble Alpes, F-38000 Grenoble, France, CEA, LETI, MINATEC Campus, F-38054 Grenoble, France.
[4] CNRS, CEMHTI UPR3079, Univ. Orléans, F-45071 Orléans, France.
[5] Univ. Grenoble Alpes, Lab. LTM (CEA-LETI/Minatec), 38000 Grenoble, France

Email : mathias.alemany@st.com

Abstract.
In this work, we report on the PAS characterization of sintered HfO_2 bulk ceramic and HfO_2 layers deposited with various methods on a silicon substrate with a layer thickness ranging from 25 to 100 nm. PAS measurements are sensitive to the deposition process type and the post-deposition annealing. Chemical and structural characterisations have been performed on the same samples. The PAS results are discussed regarding to the material defects of the different layers. In addition, a built-in electrical field induced by charged defects located at the HfO_2/Si interface as well as in the HfO_2 layer must be taken into account in the PAS data fitting. Both non-contact internal electrical field measurements and internal electrical field simulations support the PAS finding.

1. Introduction

Due to aggressive scaling for MOS devices, the transistors gate length drop requires new materials introduction. For example, high-k dielectrics (HfO_2) and metals (TiN) are used in transistor generations embedding High-k Metal Gate (HKMG) stacks, raising new issues such as shifts in transistor threshold voltages [1]. Oxygen vacancies in both HfO_2 and SiO_2 are usually invoked to explain this shift [2]. The activation spike annealing causes charged oxygen vacancies creation in high-k material, resulting in the formation of a dipole at the high-k/metal interface [3]. This dipole causes the Fermi level pinning phenomenon, responsible for the threshold voltage shift in HKMG devices [3, 4]. In addition, this shift is enhanced by oxygen vacancies creation in SiO_2 interfacial layer [5]. To asses these mechanisms, techniques capable of characterizing oxygen vacancy density in the HKMG stacks for 14 and 10 nm nodes are required. Today, two techniques are envisioned to reach these requirements: Positron Annihilation Spectroscopy (PAS) known as the most sensitive characterization method of vacancy nature and concentration in solids [6] and Electron Energy Loss

Spectroscopy (EELS) that is potentially sensitive to oxygen vacancies with a spatial resolution compatible with the dimensions of the HKMG structures [7].

Today, PAS is intensively used to characterize vacancies in diverse materials but only few studies are dedicated to high-k dielectrics [8]. Nevertheless, Uedono et al. worked on thin 3 nm HfO_2 and HfSiON layers and highlighted the existence of electric fields in the silicon substrate, near interface with HfO_2. They suggested the presence of negative charges in HfO_2 before deposition of TiN, and positive charges in HfO_2 after deposition of metal alloy and they proposed that TiN could act as a catalyst for oxygen vacancies formation. However, Uedono et al. don't observe oxygen vacancies, and suggest existence of void defects wider than vacancies.

In this paper, a slow positron beam coupled with a Doppler broadening spectrometer (DBS) has been used to study vacancy defects in HfO_2 layers on silicon. First results on PAS capabilities in this configuration are presented and discussed in terms of identification of charged defects.

2. Experimental details

2.1. Samples elaboration and characterisation

In order to assess the annihilation characteristics of the HfO_2 crystalline structure and to identify those due to oxygen vacancy, different deposition techniques have been used. HfO_2 layers with thickness ranging from 10 to 100 nm, as measured by spectroscopic ellipsometry and by SEM imaging, have been deposited on p-type 100-oriented Si substrates (B doped at ≈ 2.10^{15} cm^{-3}). An interfacial layer (IL) of native silicon oxide is located between HfO_2 layers and substrate. This IL presents a typical thickness ranging from 0.5 to 2 nm. For thick layers, Physical Vapor Deposition (PVD) technics have been used. Sputtering of an Hf target within an Ar/O_2 plasma has been used to deposit layers on 300°C heated substrates with thicknesses ranging from 25 to 100 nm. In addition, Atomic Layer Deposition (ALD) films of 10, 25 and 50 nm thickness, closer to the thickness used in microelectronic devices, were grown at 300°C using $HfCl_4$ and H_2O precursors. After deposition, spike annealing under low N_2 pressure at 900°C has been used to induce either layer densification or oxygen vacancies creation.

2.2. PAS: Doppler broadening spectroscopy (DBS)

In this work, the DBS system is a standard gamma-spectroscopy system equipped with a high purity germanium detector that offers a high energy resolution (<1.3 keV at 511 keV) and a high efficiency (>25% at 1.33 MeV). The positron emitted from a ^{22}Na radioactive source are first converted in a mono-energetic beam using a 5 µm thick tungsten foil and then accelerated at a kinetic energy ranging from 0.2 to 25 keV. The flux is ~10^5 cm^{-2} s^{-1}. The momentum distribution of the annihilated (e^+, e^-) pairs is measured at 300 K by recording the Doppler broadening of the 511 keV annihilation line. It is characterized by the low S and the high W momentum annihilation fractions in, respectively, the momentum windows (0–|2.80|×$10^{-3}m_0c$) and (|10.61|–|26.35| ×$10^{-3}m_0c$), where m_0 is the rest mass of the electron and c the speed of light. The S fraction corresponds essentially to annihilations with low momentum electrons, thus more predominantly with valence electrons. The W fraction corresponds to annihilations with high momentum electrons, thus it is essentially related to positron annihilations with core electrons. The S and W fractions are extracted from the DBS measurements acquired at energies ranging from 0.2 to 25 keV with step increasing from 0.2 to 1 keV. The positron implantation depth profile can be calculated (p. 33 in [9]), and broadens with positron energy. For the 0.2-25 keV energy range, the first 8 µm in bulk silicon can be probed. The probing depth resolution depends on the positron energy and on its mobility in the sample after kinetic energy loss, mobility influenced by trap concentration and/or by a possible electric field. Thus each point of the $S(E)$ curves results from the positron interaction on a depth section of the sample that can be larger than the HfO_2 layer thickness. Therefore fitting with VEPFIT program [10] is used to extract from experimental curves the S and W values as a function of depth. The VEPFIT program considers that the sample is made of one or several homogenous layers of material with specific annihilation characteristics. It takes into account the implantation and diffusion properties of positron in the different layers. VEPFIT supplies

information about *S*, *W*, thickness, the positron effective diffusion length L^+ and the electric field of each layer.

3. Results and discussion

Figure 1.a, shows measured *S*(*E*) curves for different PVD layers of HfO_2 and for a hot sintered bulk ceramic hafnia. For each films *S* first decreases quickly up to approximately 1.5 or 3 keV. Then it increases monotonically towards values very close to the ones reported for annihilation characteristics in the Si lattice [11] when the positron energy becomes higher than 1.5 keV or 4 keV according to the thickness of the HfO_2 layer. This variation is due to the increasing of annihilation probability in the Si substrate as the positron beam energy increases. As the thickness of the layers decreases the substrate characteristic values are reached for lower positron energy. For the 100 nm thick film, *S* parameter remains nearly constant in the 1-4 keV energy range. Compared to bulk hafnia curve, this *S* values are close to the annihilation characteristics of a bulk HfO_2. For the 25 nm thick film, the steady area on *S* curve disappears in favor of a "valley" feature for 1-2 keV energy range. This result is consistent with the corresponding implantation profiles that show a 1-3 keV range governed by the DBS characteristics of HfO_2 but this imply for thickness lower of 25 nm, the HfO_2 contribution is embedded in surface and Si contribution.

The *S*-*W* plots (figure 1.b) show for all PVD HfO_2/Si structures, a monotone and linear decrease between (*S*,*W*) values of Si and values of HfO_2 called $D_{Si/HfO2}$ and deviation from this line for SW points measured in the steady state area for the 50 and 100 nm layers, suggesting that vacancy type defects are detected in the HfO_2 layers.

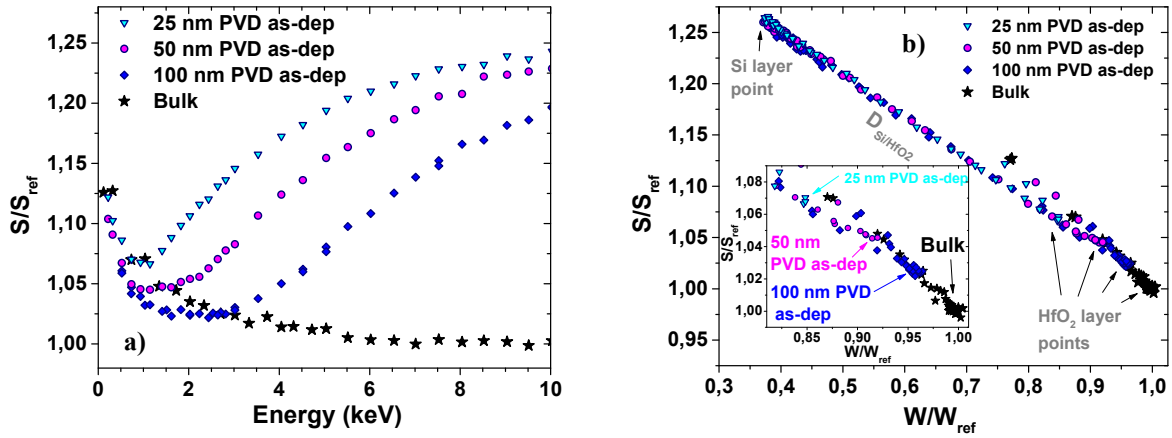

Figure 1. *S* parameter as function of incident positron energy (a) and *S*-*W* plot, with a zoomed region (b) in as-deposited PVD HfO_2/Si structures with HfO_2 thickness ranging from 25 to 100 nm compared to bulk HfO_2.We use S and W of bulk hafnia as S_{ref} and W_{ref}, with $S_{ref} = 0.3606$ and $W_{ref} = 0.0900$.

In Figure 2.a, *S* curves are plotted for the as-deposited ALD 50 nm thick layer compared to PVD one. The *S* steady state energy range is the same for both type of layers and the *S* parameter value is higher for ALD layer than for the PVD one. In the *S*-*W* plot (fig. 2.b) it has to be noticed that the ALD HfO_2/Si structure points don't follow the $D_{Si/HfO2(i)}$ line suggesting a higher initial defect concentration in ALD than in PVD layers. An explanation could be that the ALD process is usually optimized for 1-10 nm range thicknesses.

After annealing, 50 nm ALD layer shows an increase of the *S* value in the lower energy range as indicated in Figure 2.a. Moreover, the overall shape of the curves is significantly modified and very steady *S* and *W* values appear in the 1-5 keV energy range, with a slower evolution towards the Si substrate *S* characteristics. It's important to clarify that there is no modification in film thickness. According to the implantation depth profile simulation, we can assess the existence of an electric field at the ALD HfO_2/Si interface or in the HfO_2 layer that induces a shift of the DBS curves towards the

high energy range. This suggests the existence of charged defects in HfO_2, or at the HfO_2/Si interface created during annealing [3].

We compare a 10 nm as-deposited ALD thin film with 50 nm ALD ones (see fig. 2.a and 2.b). According to positron implantation profile calculation, a 10 nm thick film should be probed for energy below 1 keV. In this energy range the fraction of annihilation at the surface is high. As observed for 50 nm ALD layer (ii), the SW points measured in the as-deposited 10 nm layer are aligned on a new straight line $D_{Si/HfO2(iv-a)}$ with a lower slope than the $D_{Si/HfO2(i)}$ line. This shift suggests a non-negligible influence of silica interfacial layer between HfO_2 film and silicon substrate due to the presence of an electric field in HfO_2 or in depletion area of the substrate, as mentioned by Uedono et al [8]. This hypothesis seems supported by the behavior shown in Figure 2 for annealed 10 nm thick ALD layer where the *S-W* slope ($D_{Si/HfO2(v)}$) is similar to the $D_{Si/HfO2(iii)}$ line. This behavior suggests an electrical field modification in the stack due to charge creation induced by annealing.

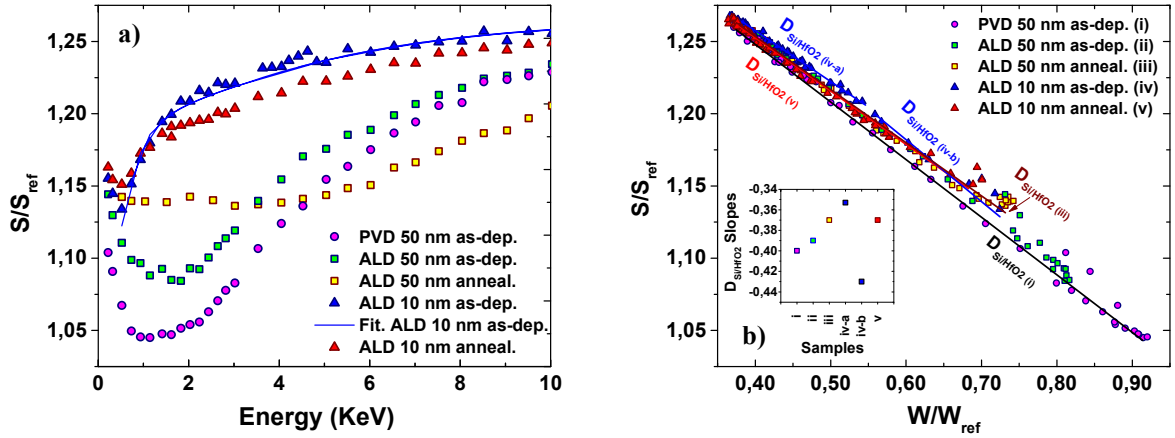

Figure 2. *S* parameter as function of incident positron energy (a) and *S-W* plot (b) in as-deposited and annealed ALD HfO_2/Si structures with 10 and 50 nm HfO_2layer thickness compared to as-deposited 50 nm PVD HfO_2/Si, all samples are numbered from (i) to (v) on legend. All $D_{Si/HfO2}$ slopes are represented as function of samples numbers on the left of figure 2 (b).

To evidence this charge creation or modification during annealing, electrical measurements have been performed using Corona Oxide Characterization of Semi-Conductors (COCOS) [12], a non-contact method, on 10 nm samples. Negatives charges are detected in the as-deposited sample, with a density of 2×10^{11} cm^{-2}. After annealing, COCOS measurements reveal positive charges with a larger density (×3) as observed in some studies [1-3]. As COCOS measurement has no depth resolution, we assume that charges are created near the interfaces in accordance with previous works [1, 3, 4]. The electric field induced by the measured charge density in the 10 nm HfO_2/Si structure has been calculated using UTOX, a Poisson solver developed at STMicroelectronics [13]. The simulation, with parameters indicated in Figure 3, results in a positive (directed towards the HfO_2/Si interface) and constant electric field, E_{HfO2}, of ≈ 3 kV/cm in HfO_2, a negative electric field E_{IL} in SiO_2 interfacial layer of ≈ 0.7 kV/cm, and a weaker negative electric field E_{Si} in the Si substrate. The E_{Si} module vanishes over a length of ≈ 200 nm. In the following we have approximated E_{Si} by a constant value of -100 V/cm over 200 nm in the Si substrate. For the annealed sample case, positive charges are imposed in hafnia (not shown), the simulation results in an inverted electric fields configuration with in a negative E_{HfO2} and a positive E_{Si}.

Injecting this value of the electric field in VEPFIT, the best fit of *S* curves found for the 10 nm as-deposited ALD sample is shown in Figure 2.a. It is obtained for an E_{HfO2} value of about 400 V/cm and the 50 V/cm for E_{IL} in SiO_2 interfacial layer, which is an order of magnitude smaller than the 3 kV/cm for E_{HfO2}, and the 0.7 kV/cm for E_{IL} calculated using UTOX. Nevertheless, the developed model is in agreement with COCOS measurements for as-deposited sample, and with Uedono et al. results for the electric field in Si [8].

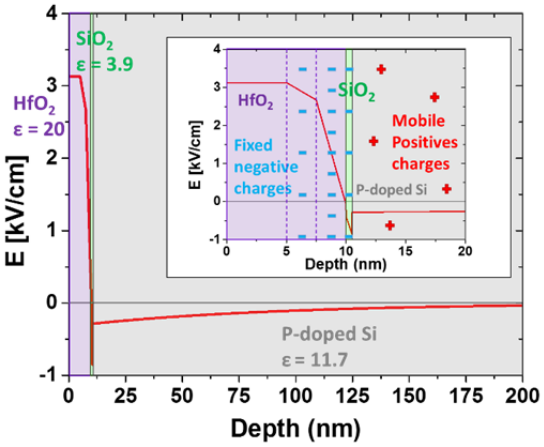

Figure 3. UTOX electric field simulation on 10 nm as-deposited layer assuming that the negative charges detected using the COCOS technique are located in HfO_2, close to the interface. Mobile positive charges in Si are attracted by fixed negative charges in HfO_2.

For the annealed sample, data fitting by VEPFIT does not allow to obtain realistic S and W values regardless of free or imposed electric fields parameters reflecting COCOS measures. Theses unrealistic S and W found during data fitting probably can highlight VEPFIT limitation concerning negative E_{HfO2} or positive E_{Si} presence. On the other hand, alternative electric fields configurations reflecting positive charges in hafnia than simulated previously, can exist. In the future more realistic charge distributions in HfO_2 will be tested in order to obtain a better agreement for the as-deposited 10 nm specimen. It is necessary to investigate on hypothetical VEPFIT limitation and to rebuild alternative charge distribution and electric field configuration model for annealed 10 nm sample.

4. Conclusion

Doppler broadening measurements performed with a slow positron beam have shown an effective sensitivity to the properties of HfO_2 layers down to a thickness of 10 nm. The qualitative analysis of the DBS curves show that the void defect concentration depends on the deposition process of the layer and it changes after annealing. The as-deposited ALD material is revealed to include more defects than the PVD one due to the out-of-range thickness for the ALD process. In addition, for ALD layers the defects concentration is higher after annealing than in the as-deposited state. The role of a built-in electrical field related to charged defects at the HfO_2/Si interface or in the HfO_2 layer is highlighted through comparison with electrical measurement by COCOS and electric field simulation. However, a quantitative analysis based on data reduction using complete DBS simulations is still limited by the lack of knowledge of the annihilation characteristics in the HfO_2 material. Significant information about defect parameters could be brought by DFT simulation. Also, to fulfill the nano-electronic specifications, coupling PAS with EELS-TEM and cathodoluminescence analyses is mandatory.

Acknowledgment

This work was supported by the National Research Agency (ANR) through the French "Recherche Technologique de Base" Program. The experiments were performed in the frame of the joint development program with STMicroelectronics and the Nanocharacterisation platform (PFNC) at MINATEC. We warmly thank A. Roule, H. Grampeix from LETI for providing ALD and PVD deposition.

References

[1] Shiraishi K, Yamada K,Torii K, Akasaka Y, Nakajima K, Konno M, Chikyow T, Kitajima H, Arikado T and Nara.Y 2006 *Thin Solid Films* **508** 305
[2] Guha S and Narayanan V 2007 *Physical Review Letters* **98** 196101
[3] Kechichian A, Barboux P, and Gros-Jean 2013 M *ECS Transactions* **58** 325
[4] Robertson J, Sharia O, and Demkov A A 2007 *Applied Physics Letters* **91** 132912

[5] Bersuker G, Park C S, Wen H C, Choi K, Price J, Lysaght P, Tseng H H, Sharia O, Demkov A, Ryan J T and Lenahan P 2010 *IEEE Transaction on Electron Devices* **57** 2047
[6] Uedono A, Naito T, Otsuka T, Ito K, Shiraishi K, Yamabe K, Miyazaki S, Watanabe H, Umezawa N, Chikyow T, Ohdaira T, Suzuki R, Akasaka Y, Kamiyama S, Nara Y and Yamada K 2007 *Japanese Journal of Applied Physics* **46** 3214
[7] Calka P, Martinez E, Delaye V, Lafond D, Audoit G, Mariolle D, Chevalier N, Granpeix H, Cagli C, Jousseaume V and Guedj C 2013 *Nanotechnology* **24** 085706
[8] Uedono, Naito T, Otsuka T, Ito K, Shiraishi K, Yamabe K, Miyazaki S, Watanabe H, Umezawa N, Chikyow T, Akasaka Y, Kamiyama S, Nara Y, Yamada K 2006 *Journal of Applied Physics* **100** 034509
[9] Krause-Rehberg R and Leipner H S 1999 *Positron Annihilation in Semiconductors: Defect Studies*, (Berlin: Springer-Verlag) p 33
[10] Van Veen A, Schut H, De Vries J, Hakvoort R A and Ijpma M R 1991 *SLOPOS 4 (Ontario) AIP Conf. Proc.* **218** 171
[11] Kauppinen H, Corbel C, Liszkay L, Laine T, Oila J, Saarinen K, Hautojärvi P, Barthe M F and Blondiaux G 1997 *Journal of Physics: Condensed Matter* **9** 10595
[12] Wilson M, Lagowski J, Jastrzebski L, Savtchouk A and Faifer V 2001 *Conf.Characterization and Metrology for ULSI Technology 2000 (Gaithersburg) AIP Conf. Proc.* **550** 220
[13] Garetto D, Rideau D, Dornel E, Tavernier C, Leblebici Y, Schmid A, Jaouen H 2011. *Proc. NSTI Nanotech 2011 (Boston),* vol 2 607